A Unilateral Parametric Amplifier

HELMUT E. BRENNER, MEMBER, IEEE

***Abstract*—A theoretical investigation of a unilateral parametric amplifier using two varactor diodes indicates an improvement of unilateral stability over already existing types. A circuit is suggested which uses lower sideband idler energy for achieving forward gain and upper sideband energy to obtain substantial reverse loss. The phases of the applied signals and of the pump at the two varactors have to be 90° out of phase to achieve unilateral operation.**

Numerical evaluation of the theoretical results for a signal frequency at 4.0 GHz and a pump frequency at 12.0 GHz, assuming a diode junction capacitance of $C_j = 0.4$ pF and a bulk resistance of $R_s = 2\Omega$ was done for several pump power levels. For 14 dB maximum forward gain, the 3 dB bandwidth of the gain versus frequency characteristic of the unilateral amplifier is about 18 percent smaller than that of the reflection type amplifier. The maximum reverse loss for these conditions is 7.3 dB. For lower forward gain the backward loss increases relatively until for very low gain values (about 1 dB) the amplifier is unconditionally stable, i.e., the backward loss is larger than the forward gain. The theoretical noise figure is about 1.95 dB at signal center frequency for 14 dB forward gain and, for ±80 MHz from the center frequency, only 0.1 dB higher than for the reflection type amplifier.

Introduction

THE IDEA of a unilateral parametric amplifier is not new. In 1961 Baldwin [1] proposed some nonreciprocal parametric-amplifier circuits, which, while not using a circulator, had properties similar to the single-port reflection amplifier with a three-port circulator. These circuits consist of two time-varying reactances with a relative phase shift of 90° between them. Also the signal is shifted by 90° at the two diodes. There is a common idler circuit for the two varactors. In the first circuit, a 3 dB directional coupler is used to split the incoming signal into two equal parts but with 90° phase difference; in the second circuit a 90° phase shift network is used for this purpose. In the common idler circuit the currents from the two diodes add up in phase when signal power enters the amplifier in the forward direction, so causing amplification of the signal. When signal power enters at the output port, the idler currents cancel, now causing a gain of slightly less than unity (insertion loss) in the reverse direction.

In 1963 Hamasaki [2] published the theory of a unilateral parametric amplifier using two diodes pumped 90° out of phase and located in a coaxial line with a separation of a quarter wavelength at signal frequency. As the diode separation has to be an integral number of half wavelengths for the idler frequency to achieve unilateral amplification the application of this structure is restricted to certain signal-pump frequency relationships (for example 1 to 3). All those structures described above show no substantial loss in the reverse direction.

Manuscript received August 8, 1966; revised December 21, 1966.
The author is with Bell Telephone Laboratories, Inc., Murray Hill, N. J.

The purpose of this paper is to investigate a unilateral structure which uses not only a common circuit for the idler frequency but another one for the upper sideband frequency. Other nonreciprocal circuits employing upper sideband energy were described in 1960 by Kamal [3] and by Adams [4] and in 1963 by Maurer and Löecherer [5] and by Anderson and Auckland [6]. The purpose of the upper sideband is to present a positive resistance to a signal wave entering the amplifier in the reverse direction, resulting in reverse loss. In addition, the presented configuration does not restrict the design of unilateral amplifiers to certain frequency relationships.

General Principles of the Amplifier

The basic configuration of the unilateral amplifier circuit presented in this paper is shown in Fig. 1. A signal wave entering the 3 dB coupler at port 1 is split up into two waves of equal amplitude but with a relative phase difference of 90° between them. These two waves leave the coupler at the ports 2 and 3, the wave at port 2 leading the one at port 3 by 90°. Also the phases of the pump at the varactors V_{I} and V_{II} differ by 90° as shown in Fig. 1. From this the relative phases of signal, pump, and the generated idler and upper sideband energies are as follows for resonance:

at	V_{I}	V_{II}
signal center frequency (f_{s0})	$\omega_{s0}t$	$\omega_{s0}t-90°$
pump frequency (f_p)	$\omega_p t$	$\omega_p t+90°$
idler center frequency (f_{i0})	$\omega_{i0}t$	$\omega_{i0}t+180°$
upper sideband center frequency (f_{u0})	$\omega_{u0}t$	$\omega_{u0}t$

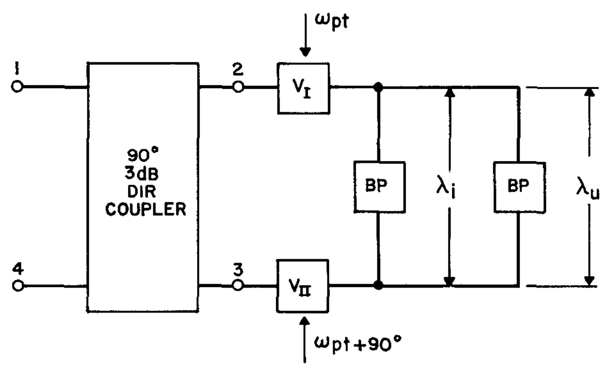

Fig. 1. Schematic diagram of unilateral amplifier.

Two lossless waveguides together with lossless bandpass filters for f_i and f_u connect the varactors. For both frequencies the electrical length of the interconnecting network is one wavelength at the respective band center frequencies. The waves originated at the individual varactors propagate into the waveguides and superpose. Because the electrical distance is one wavelength, the phase of a specific wave is identical at both varactors. That means, for example for f_{i0} that the phases of both idler waves are 180° out of phase at both varactors. But as they are coming from opposite directions, the amplitudes add up and energy is dissipated at the idler frequency in the bulk resistances R_s of both varactors, thus creating a negative resistance and amplification for the signal wave. For the upper sideband the opposite is the case; the amplitudes of the two generated waves cancel at the varactors, therefore no energy is dissipated at f_{u0} and the effect of the upper sideband is zero. The amplified and reflected signal waves re-enter the 3 dB coupler at the ports 2 and 3. Because of their phase relationship all the energy leaves the coupler at port 4.

When a signal wave is entering the amplifier from the reverse direction, i.e., at port 4, the phase relationships of the four frequencies are now different:

at	V_I	V_{II}
signal center frequency (f_{s0})	$\omega_{s0}t - 90°$	$\omega_{s0}t$
pump frequency (f_p)	$\omega_p t$	$\omega_p t + 90°$
idler center frequency (f_{i0})	$\omega_{i0}t + 90°$	$\omega_{i0}t + 90°$
upper center sideband frequency (f_{u0})	$\omega_{u0}t - 90°$	$\omega_{u0}t + 90°$

In this case the amplitudes of the upper sideband waves add up at the varactors and the idler waves cancel. Energy is dissipated at f_u, presenting a positive resistance to the signal waves. The effect of the idler is now zero. The signal waves are reflected and attenuated and leave the amplifier at port 1.

This shows that the circuit in Fig. 1 represents a nonreciprocal device which amplifies in the forward direction and attenuates in the reverse direction.

Derivation of the Impedance and Scattering Matrix of the Amplifier

The points of maximum interest in the analysis of the amplifier are matching at the input and output ports of the 3 dB coupler, the forward gain characteristics, the reverse loss, and the noise figure.

In order to investigate these characteristics, the amplifier is divided into five parts: the two pumped varactors, the two interconnecting lines for the idler and upper sideband waves, respectively, and the 3 dB coupler.

First the impedance matrices for the two varactors shall be presented. We assume a small signal theory with open circuited unwanted harmonics. The pumped elastance $S(t)$ shall be represented by an average elastance S_0 and the half amplitude of the first harmonic of the Fourier expansion of $S(t)$ equal to S_1. At resonance S_0 shall be tuned out by the inductances L_s, L_i, and L_u in the signal, idler, and upper sideband circuits, respectively. The bulk resistance R_s is responsible for thermal noise with open circuit noise voltages E_{ns}, E_{ni}, and E_{nu}, respectively. The two varactors V_I and V_{II} are assumed to be identical in S_0, S_1, and R_s. The complex variables for voltages and current of V_I shall be denoted without a prime, those of V_{II} with a prime. As the exact derivation of the frequency dependence of the characteristics is extremely tedious, we shall restrict ourselves to small frequency deviations $\Delta\omega$ from the resonance frequencies. Therefore a linearized theory shall be used, neglecting all terms with higher than first order in $\Delta\omega$ for the determination of the coefficients of the impedance matrix. The fact that the phase of the pumped elastance of V_{II} is 90° ahead of V_I shall be expressed by setting $S_{1_{II}} = jS_{1_I} = jS_1$, S_1 being the complex half amplitude of the elastance variation at V_I.

With these assumptions and referring to Fig. 2 and Penfield and Rafuse [7] the matrix equations for the voltages and currents of the two pumped varactors including tuning inductances and noise sources become:

$$
\begin{aligned}
V_i^* &= I_i^*(R_s + j\Delta\omega X_i) - I_s \frac{jS_1^*}{\omega_{s0}}\left(1 - \frac{\Delta\omega}{\omega_{s0}}\right) + E_{ni}^* \\
V_s &= I_i^* \frac{jS_1}{\omega_{i0}}\left(1 + \frac{\Delta\omega}{\omega_{i0}}\right) + I_s(R_s + j\Delta\omega X_s) \\
&\quad - I_u \frac{jS_1^*}{\omega_{u0}}\left(1 - \frac{\Delta\omega}{\omega_{u0}}\right) + E_{ns} \\
V_u &= - I_s \frac{jS_1}{\omega_{s0}}\left(1 - \frac{\Delta\omega}{\omega_{s0}}\right) + I_u(R_s + j\Delta\omega X_u) + E_{nu}
\end{aligned}
\tag{1a}
$$

$$
\begin{aligned}
V_i' &= I_i'^*(R_s + j\Delta\omega X_i) - I_s' \frac{S_1^*}{\omega_{s0}}\left(1 - \frac{\Delta\omega}{\omega_{s0}}\right) + E_{ni}'^* \\
V_s' &= - I_i'^* \frac{S_1}{\omega_{i0}}\left(1 + \frac{\Delta\omega}{\omega_{i0}}\right) + I_s'(R_s + j\Delta\omega X_s) \\
&\quad - I_u' \frac{S_1^*}{\omega_{u0}}\left(1 - \frac{\Delta\omega}{\omega_{u0}}\right) + E_{ns}' \\
V_u' &= + I_s' \frac{S_1}{\omega_{s0}}\left(1 - \frac{\Delta\omega}{\omega_{s0}}\right) + I_u'(R_s + j\Delta\omega X_u) + E_{nu}'.
\end{aligned}
\tag{1b}
$$

In these equations $\Delta\omega X_s$, $\Delta\omega X_i$, and $\Delta\omega X_u$ represent the reactance slopes of the three circuits at their respective resonance frequencies. The slope of the signal circuit is

$$
j(\omega_{s0} + \Delta\omega)L_s - \frac{jS_0}{(\omega_{s0} + \Delta\omega)} \doteq j\omega_{s0}L_s + j\Delta\omega L_s - j\frac{S_0}{\omega_{s0}}\left(1 - \frac{\Delta\omega}{\omega_{s0}}\right).
$$

For

$$
\omega_s = \omega_{s0} \cdots j\omega_{s0}L_s - j\frac{S_0}{\omega_{s0}} = 0,
$$

therefore,

$$
j\Delta\omega\left(L_s + \frac{S_0}{\omega_{s0}^2}\right) = j\Delta\omega X_s
$$

is left. Similarly, for the idler circuit

$$
X_i = L_i + \frac{S_0}{\omega_{i0}^2}, \quad \text{and} \quad X_u = L_u + \frac{S_0}{\omega_{u0}^2}.
$$

The two-port equations for the waveguides with the length l_i and l_u, respectively, connecting the two varactors are with the notations of Fig. 3

$$V_{i,u} = V_{i,u}' \cos\frac{2\pi l_{i,u}}{\lambda_{i,u}} + jI_{i,u}'Z_{i,u} \sin\frac{2\pi l_{i,u}}{\lambda_{i,u}}$$

$$I_{i,u} = -I_{i,u}' \cos\frac{2\pi l_{i,u}}{\lambda_{i,u}} - j\frac{V_{i,u}'}{Z_{i,u}} \sin\frac{2\pi l_{i,u}}{\lambda_{i,u}}. \quad (2a)$$

Substituting $2\pi l/\lambda$ by $\omega l/v = (\omega_0 l/v) + (\Delta\omega l/v)$ and remembering that the resonance length shall be one wavelength, we get $2\pi l/\lambda = 2\pi + (\Delta\omega l/v)$. $v \cdots$ propagation phase velocity of the wave under consideration.

With a linear approximation in $\Delta\omega$ of the expressions, (2a) becomes

$$V_i = V_i' - jI_i'Z_i\frac{\Delta\omega l_i}{v_i}$$

$$I_i = -I_i' + j\frac{V_i'}{Z_i}\frac{\Delta\omega l_i}{v_i} \quad (2b)$$

and

$$V_u = V_u' + jI_u'Z_u\frac{\Delta\omega l_u}{v_u}$$

$$I_u = -I_u' - j\frac{V_u'}{Z_u}\frac{\Delta\omega l_u}{v_u} \quad (2c)$$

for the idler and upper sideband.

By eliminating the idler and upper sideband currents and voltages using (1a), (1b), (2b), and (2c) the impedance matrix of the amplifier without the 3 dB coupler can be presented in the following form

$$V_s = Z_{11}I_s + Z_{12}I_s' + V_{sn}$$

$$V_s' = Z_{21}I_s + Z_{22}I_s' + V_{sn}'. \quad (3)$$

V_{sn} and V_{sn}' represent the open-circuit noise voltages at the signal ports of V_{I} and V_{II}, respectively, including the effects of E_{ns}, E_{ns}', E_{ni}, E_{ni}', E_{nu}, and E_{nu}'. The results show that there is a symmetry $Z_{11} = Z_{22}$ and $Z_{12} = -Z_{21}$ which is exact for resonance and holds for the linear approximation assuming $\Delta\omega \ll \omega_{s0}$.

The next step for the derivation of our amplifier characteristics is to connect the s and s' ports with the proper ports of the 3 dB coupler. With the notation of Fig. 4 the scattering waves may be expressed as:

$$a = \frac{1}{2}\left(\frac{V}{\sqrt{Z}} - \sqrt{Z}\,I\right)$$

$$b = \frac{1}{2}\left(\frac{V}{\sqrt{Z}} + \sqrt{Z}\,I\right). \quad (4)$$

Connecting (3) and (4) the scattering variables at the two varactor ports become:

$$a_s = \frac{1}{2}\left[\frac{1}{\sqrt{Z}}(Z_{11}I_s + Z_{12}I_s' + V_{sn}) - \sqrt{Z}\,I_s\right]$$

$$b_s = \frac{1}{2}\left[\frac{1}{\sqrt{Z}}(Z_{11}I_s + Z_{12}I_s' + V_{sn}) + \sqrt{Z}\,I_s\right] \quad (5a)$$

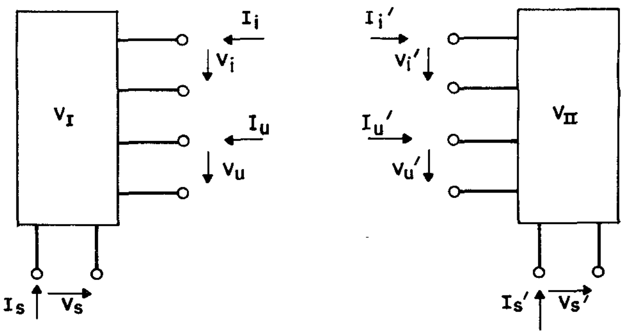

Fig. 2. The two varactor pairs V_{I} and V_{II} as three-port networks.

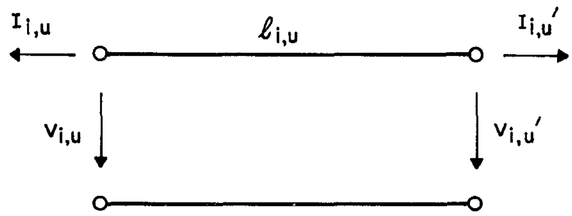

Fig. 3. The lines connecting the two varactor pairs.

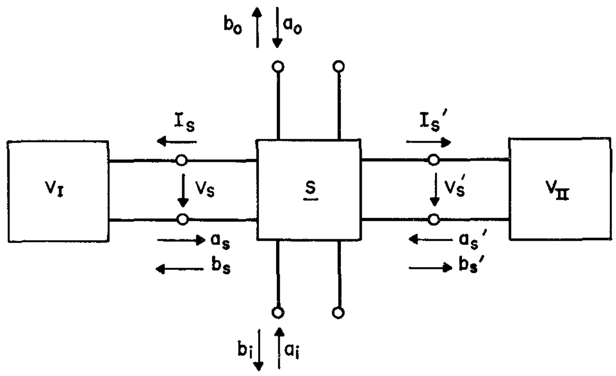

Fig. 4. Network diagram of the two varactor pairs V_{I} and V_{II} and the 3 dB coupler. The interconnecting circuits for idler and upper sideband are not shown.

$$a_s' = \frac{1}{2}\left[\frac{1}{\sqrt{Z}}(Z_{21}I_s + Z_{22}I_s' + V_{sn}') - \sqrt{Z}\,I_s'\right]$$

$$b_s' = \frac{1}{2}\left[\frac{1}{\sqrt{Z}}(Z_{21}I_s + Z_{22}I_s' + V_{sn}') + \sqrt{Z}\,I_s'\right]. \quad (5b)$$

Z is the characteristic impedance of the coupler and the signal lines. The scattering matrix of the 3 dB coupler is

$$b_i = 0 + \frac{j}{\sqrt{2}}e^{-j\phi}a_s + \frac{1}{\sqrt{2}}e^{-j\phi}a_s' + 0$$

$$b_s = \frac{1}{\sqrt{2}}e^{-j\phi}a_i + 0 + 0 + \frac{1}{\sqrt{2}}e^{-j\phi}a_0$$

$$b_s' = \frac{1}{\sqrt{2}}e^{-j\phi}a_i + 0 + 0 + \frac{j}{\sqrt{2}}e^{-j\phi}a_0$$

$$b_0 = 0 + \frac{1}{\sqrt{2}}e^{-j\phi}a_s + \frac{j}{\sqrt{2}}e^{-j\phi}a_s' + 0. \quad (6)$$

Using (5) and (6) a tedious elimination process gives the two-port scattering matrix of the whole amplifier.

$$\begin{aligned} b_i &= S_{ii}a_i + S_{i0}a_0 + b_{in} \\ b_0 &= S_{0i}a_i + S_{00}a_0 + b_{on}. \end{aligned} \tag{7}$$

b_{in} and b_{on} are noise waves leaving the amplifier at the in and out ports. The scattering coefficients can be expressed in terms of the coefficients of the impedance matrix. In connection with the impedance coefficients the characterization of the amplifier is possible. S_{ii} and S_{00} are the voltage reflection coefficients at the input and output, respectively, $|S_{0i}|^2$ is the power gain (PG) in the forward direction, and $|S_{i0}|^2$ is the power loss (PL) in the reverse direction. From the identities $Z_{11}=Z_{22}$ and $Z_{12}=-Z_{21}$, for resonance and small deviations from resonance, it can be shown that $S_{ii}=S_{00}\equiv 0$. That means in the vicinity of resonance the amplifier is matched at the input and output ports.

From these facts the expression for the noise figure can be written as

$$F = 1 + \frac{|b_{on}|^2}{kTB\,|S_{0i}|^2}. \tag{8}$$

The evaluation of S_{i0}, S_{0i}, b_{in}, and b_{on} is rather tedious. On the other hand, the fact that there are no reflections at the input and output of the amplifier indicates that the ports 2 and 3 of the 3 dB coupler are terminated by identical impedances, i.e., signal waves from these ports maintain their 90° phase shift between them also after being reflected and amplified or attenuated at these terminations. Therefore using the relationship $I_s' = -jI_s$ in (3) in connection with the expressions obtained for the impedance matrix yields the impedances $Z_f = Z_f'$ which the varactors V_{I} and V_{II} present to the signal waves in the forward direction.

$$\begin{aligned} Z_f = \Bigg[R_s - \frac{|S_1|^2}{R_s\omega_{s0}\omega_{i0}} + \frac{|S_1|^2\Delta\omega}{\omega_{s0}} &\cdot \left(\frac{1}{R_s\omega_{s0}\omega_{i0}} - \frac{1}{R_s\omega_{i0}^2} \right) \Bigg] \\ + j\Bigg[\Delta\omega X_s + \frac{|S_1|^2\Delta\omega}{\omega_{s0}} &\cdot \left(\frac{X_1}{R_s^2\omega_{i0}} + \frac{l_u}{2\omega_{u0}Z_u v_u} + \frac{Z_i l_i}{2R_s^2\omega_{i0}v_i} \right) \Bigg]. \end{aligned} \tag{9}$$

Similarly, the varactor impedances $Z_r = Z_r'$, for the reverse direction, can be obtained by the relation $I_s' = jI_s$

$$\begin{aligned} Z_r = &\left[R_s + \frac{|S_1|^2}{R_s\omega_{s0}\omega_{u0}} - \frac{|S_1|^2\Delta\omega}{\omega_{s0}} \left(\frac{1}{R_s\omega_{s0}\omega_{u0}} + \frac{1}{R_s\omega_{u0}^2} \right) \right] \\ &+ j\left[\Delta\omega X_s - \frac{|S_1|^2\Delta\omega}{\omega_{s0}} \left(\frac{X_u}{R_s^2\omega_{u0}} + \frac{l_i}{2\omega_{i0}Z_i v_i} + \frac{Z_u l_u}{2R_s^2\omega_{u0}v_u} \right) \right]. \end{aligned} \tag{10}$$

Now the well-known formula for the power reflection coefficient of a signal wave in a waveguide of the characteristic impedance Z terminated by the impedance Z_f or Z_r can be used to obtain equations for the power gain and power loss of the amplifier.

$$\mathrm{PG} = \left| \frac{Z - Z_f}{Z + Z_f} \right|^2 \tag{11}$$

$$\mathrm{PL} = \left| \frac{Z - Z_r}{Z + Z_r} \right|^2 \tag{12}$$

With (9) and (10) these become

$$\mathrm{PG} = \frac{\left[Z - R_s + \frac{|S_1|^2}{R_s\omega_{s0}\omega_{i0}} - \frac{|S_1|^2\Delta\omega}{\omega_{s0}} \left(\frac{1}{R_s\omega_{s0}\omega_{i0}} - \frac{1}{R_s\omega_{i0}^2} \right) \right]^2 + \left[\Delta\omega X_s + \frac{|S_1|^2\Delta\omega}{\omega_{s0}} \left(\frac{X_i}{R_s^2\omega_{i0}} + \frac{l_u}{2\omega_{u0}Z_u v_u} + \frac{Z_i l_i}{2R_s^2\omega_{i0}v_i} \right) \right]^2}{\left[Z + R_s - \frac{|S_1|^2}{R_s\omega_{s0}\omega_{i0}} + \frac{|S_1|^2\Delta\omega}{\omega_{s0}} \left(\frac{1}{R_s\omega_{s0}\omega_{i0}} - \frac{1}{R_s\omega_{i0}^2} \right) \right]^2 + \left[\Delta\omega X_s + \frac{|S_1|^2\Delta\omega}{\omega_{s0}} \left(\frac{X_i}{R_s^2\omega_{i0}} + \frac{l_u}{2\omega_{u0}Z_u v_u} + \frac{Z_i l_i}{2R_s^2\omega_{i0}v_i} \right) \right]^2} \tag{13}$$

$$\mathrm{PL} = \frac{\left[Z - R_s - \frac{|S_1|^2}{R_s\omega_{s0}\omega_{u0}} + \frac{|S_1|^2\Delta\omega}{\omega_{s0}} \left(\frac{1}{R_s\omega_{s0}\omega_{u0}} + \frac{1}{R_s\omega_{u0}^2} \right) \right]^2 + \left[\Delta\omega X_s - \frac{|S_1|^2\Delta\omega}{\omega_{s0}} \left(\frac{X_u}{R_s^2\omega_{u0}} + \frac{l_i}{2\omega_{i0}Z_i v_i} + \frac{Z_u l_u}{2R_s^2\omega_{u0}v_u} \right) \right]^2}{\left[Z + R_s + \frac{|S_1|^2}{R_s\omega_{s0}\omega_{u0}} - \frac{|S_1|^2\Delta\omega}{\omega_{s0}} \left(\frac{1}{R_s\omega_{s0}\omega_{u0}} + \frac{1}{R_s\omega_{u0}^2} \right) \right]^2 + \left[\Delta\omega X_s - \frac{|S_1|^2\Delta\omega}{\omega_{s0}} \left(\frac{X_u}{R_s^2\omega_{u0}} + \frac{l_i}{2\omega_{i0}Z_i v_i} + \frac{Z_u l_u}{2R_s^2\omega_{u0}v_u} \right) \right]^2}. \tag{14}$$

For the derivation of the noise powers $|b_{on}|^2$ and $|b_{in}|^2$ similar simplifications as for the forward gain and reverse loss were used. After rather involved algebraic manipulations and using finally (8) the noise figure can be expressed as

$$F = 1 + \frac{4R_s Z \left\{ 1 + \frac{|S_1|^2}{R_s^2} \left[\frac{\Delta\omega^2}{\omega_{i0}^2} \left(\frac{X_i}{R_s} + \frac{Z_i l_i}{2R_s v_i} \right)^2 + \left(\frac{1}{\omega_{i0}} + \frac{\Delta\omega}{\omega_{i0}^2} \right)^2 \right] + \frac{|S_1|^2}{4} \left(\frac{\Delta\omega l_u}{\omega_{u0} Z_u v_u} \right)^2 \right\}}{\left[Z - R_s + \frac{|S_1|^2}{R_s\omega_{s0}\omega_{i0}} - \frac{|S_1|^2\Delta\omega}{\omega_{s0}} \left(\frac{1}{R_s\omega_{s0}\omega_{i0}} - \frac{1}{R_s\omega_{i0}^2} \right) \right]^2 + \left[\Delta\omega X_s + \frac{|S_1|^2\Delta\omega}{\omega_{s0}} \left(\frac{X_i}{R_s^2\omega_{i0}} + \frac{l_u}{2\omega_{u0}Z_u v_u} + \frac{Z_i l_i}{2R_s^2\omega_{i0}v_i} \right) \right]^2}. \tag{15}$$

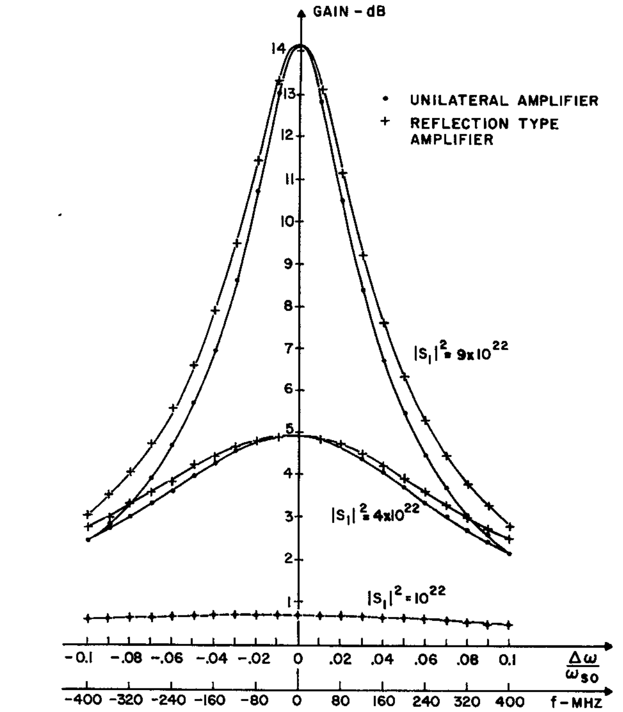

Fig. 5. Theoretical gain versus frequency characteristics of the unilateral and of the reflection type parametric amplifiers for $|S_1|^2=10^{22}$, 4×10^{22}, and 9×10^{22} (daraf)^2.

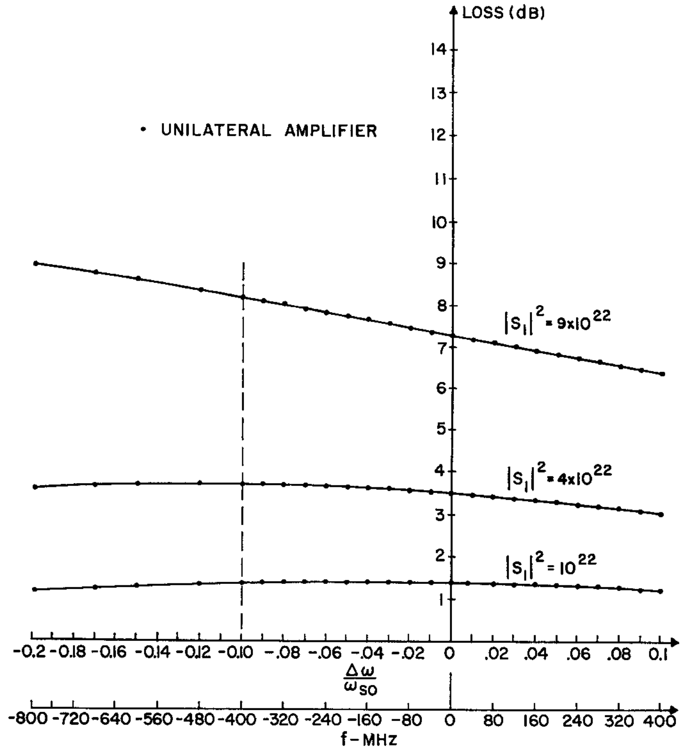

Fig. 6. Plots of the theoretical loss versus frequency characteristics of the unilateral amplifier for $|S_1|^2=10^{22}$, 4×10^{22}, and 9×10^{22} (daraf)^2.

Numerical Evaluation of the Amplifier Characteristics

Figures 5 through 7 show plots of (13), (14), and (15) for forward gain, reverse loss, and noise figure of the unilateral amplifier. For comparison the gain and noise figure of the reflection type parametric amplifier are also plotted. The following values were assumed for the constants:

$$
\begin{aligned}
Z &= Z_i = Z_u = 50\ \Omega & l_u &= 0.187 \times 10^{-2}\, m\\
R_s &= 2\ \Omega & v_i &= v_u = 3 \times 10^8\, m/s\\
X_s &= 6 \times 10^{-9}\ \Omega/s & \omega_{s0} &= 8\pi \times 10^9\, l/s\\
X_i &= 1.5 \times 10^{-9}\ \Omega/s & \omega_{i0} &= 16\pi \times 10^9\, l/s\\
X_u &= 0.375 \times 10^{-9}\ \Omega/s. & \omega_{u0} &= 32\pi \times 10^9\, l/s\\
l_i &= 0.375 \times 10^{-2}\, m. & &
\end{aligned}
$$

The frequency range was restricted to within $\Delta\omega/\omega_{s0}=\pm0.1$ not to violate the validity of the condition $|\Delta\omega|\ll\omega_{s0}$ for the approximations used in the derivations. Only for the reverse loss the curves were plotted to $\Delta\omega/\omega_{s0}=-0.2$ to get an idea of the general behavior in that range. There are three sets of curves which correspond to the values $|S_1|^2=10^{22}$, 4×10^{22}, and 9×10^{22} (daraf)^2.

For $\Delta\omega=0$, which means resonance of all circuits, the values for the gain and noise figure are the same for the unilateral and the reflection type parametric amplifier. First the gain curves in Fig. 5 shall be examined closer: the gain values at resonance for the three different pump levels are 0.7, 5.0, and 14.0 dB. Because of the frequency dependent

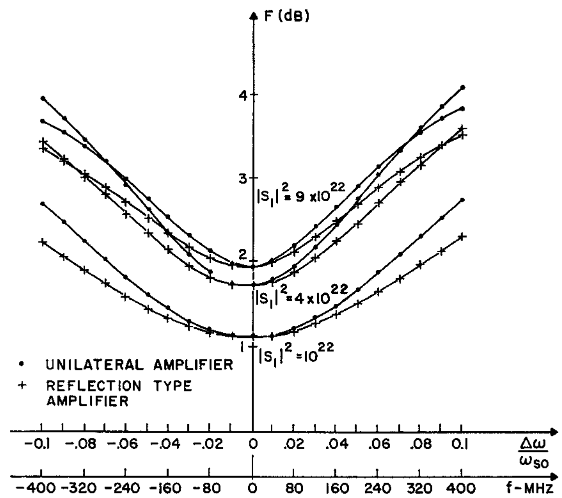

Fig. 7. Plots of the theoretical noise figure of the unilateral and of the reflection type parametric amplifiers for $|S_1|^2=10^{22}$, 4×10^{22}, and 9×10^{22} (daraf)^2.

negative resistance in the input impedance Z_f, the *maximum* gain is slightly higher and occurs for a slightly lower frequency than the resonance frequency ω_{s0}. The 3 dB bandwidth of the unilateral amplifier for the 14 dB curve is about 140 MHz, for the reflection type amplifier 170 MHz.

When the phase velocities v_i and v_u are frequency dependent as in waveguides—especially when operated close to cutoff—then the bandwidth of the unilateral amplifier will be still narrower. Figure 6 shows the graphs of the reverse loss. The curves are extremely broadband because of the small reactive term of Z_r in (14). This also makes the frequency dependent term of the real part of Z_r quite effective in such a way that the frequency for maximum loss is appreciably below ω_{s0}. For high levels of pumping, i.e., large values of $|S_1|^2$, this frequency is lower than for low pump levels. The loss values at $\Delta\omega=0$ for the three pump levels are 1.4, 3.5, and 7.3 dB, respectively, which means that only for the case of 0.7 dB forward gain there is more backward loss in dB than forward gain, i.e., only for very low gain values, where the influence of R_s becomes noticeable, the amplifier is unconditionally stable. By substituting the lossless interconnecting network by one with proper resistive loading it may be possible to make the amplifier unconditionally stable also for high forward gain.

Figure 7 shows the noise figure F versus frequency. The minimum is again a little off resonance (at a negative $\Delta\omega$) and increases with $|S_1|^2$ from 1.12 to 1.72 and 1.95 dB, respectively.

For a 400 MHz deviation from the resonance frequency the noise figure has increased between 1.25 and 1.9 dB for the reflection type amplifier and between 1.90 and 2.40 dB for the unilateral amplifier. That means that the unilateral amplifier noise figure is 0.3 to 0.5 dB higher at that frequency. Within a frequency band of ± 180 MHz from resonance the difference is maximally 0.1 dB.

Special Cases

For the resonance case, $\Delta\omega=0$, the equations for forward gain, reverse loss, and noise figure become:

$$PG = \left[\frac{Z - R_s + \dfrac{|S_1|^2}{R_s\omega_{s0}\omega_{i0}}}{Z + R_s - \dfrac{|S_1|^2}{R_s\omega_{s0}\omega_{i0}}}\right]^2 \tag{16}$$

$$PL = \left[\frac{Z - R_s - \dfrac{|S_1|^2}{R_s\omega_{s0}\omega_{u0}}}{Z + R_s + \dfrac{|S_1|^2}{R_s\omega_{s0}\omega_{u0}}}\right]^2 \tag{17}$$

$$F = 1 + \frac{4R_sZ\left[1 + \dfrac{|S_1|^2}{R_s^2\omega_{i0}^2}\right]}{\left[Z - R_s + \dfrac{|S_1|^2}{R_s\omega_{s0}\omega_{i0}}\right]^2}. \tag{18}$$

If now $|S_1|\to 0$ or $\omega_p\to\infty$

$$PG = \left[\frac{Z - R_s}{Z + R_s}\right]^2 = PL = \text{insertion loss of the varactor diode} \tag{19}$$

$$F = 1 + \frac{4R_sZ}{[Z - R_s]^2} \tag{20}$$

and for $R_s\to 0$

$$PG = PL = 1$$

$$F = 1$$

Conclusion

Theoretical investigation of the presented type of a unilateral parametric amplifier indicates little sacrifice in gain bandwidth and off-resonance noise figure in comparison to the reflection type amplifier. By using upper sideband energy, substantial reverse loss can be obtained. With the amplifier in the present configuration, the reverse loss exceeds the forward gain only for very low gain values.

Acknowledgment

The author is indebted to R. Engelbrecht and K. Kurokawa for stimulating and helpful discussions. Miss E. Murphy did the computer work for the numerical evaluation of the amplifier characteristics.

References

[1] L. D. Baldwin, "Nonreciprocal parametric amplifier circuits," *Proc. IRE (Correspondence)*, p. 1075, vol. 49, June 1961.
[2] J. Hamasaki, "A theory of a unilateral parametric amplifier using two diodes," *Bell Sys. Tech. J.*, vol. 43, pp. 1123–1147, May 1964.
[3] A. K. Kamal, "A parametric device as a nonreciprocal element," *Proc. IRE*, vol. 48, pp. 1424–1430, August 1960.
[4] D. K. Adams, "An analysis of four-frequency nonlinear reactance circuits," *IRE Trans. on Microwave Theory and Techniques*, vol. MTT-8, pp. 274–283, May 1960.
[5] R. Maurer and K. H. Löecherer, "Low-noise nonreciprocal parametric amplifier with power matching at the input and output," *Proc. IEEE*, vol. 51, pp. 1589–1598, November 1963.
[6] D. B. Anderson and J. C. Aukland, "A general catalog of gain, bandwidth and noise temperature expressions for four-frequency parametric devices," *IEEE Trans. on Electron Devices*, vol. ED-10, pp. 13–30, January 1963.
[7] P. Penfield and R. P. Rafuse, *Varactor Applications*. Cambridge, Mass.: M.I.T. Press, 1962.